Scientific Research

Structural Performance Evaluation After Cracking During the Construction of Long-Span Continuous Rigid-Frame Bridges

Jiasi Chen *, Chengyue Wang and Yin Shen

Department of Bridge Engineering, Tongji University, Shanghai 200092, China;
* Correspondence: 1150269075@qq.com

Abstract: Cracking evaluation technology during construction is crucial for evaluating the safety performance of long-span bridges and for selecting remedial measures. In this paper, by focusing on the cracking of pier cap block 0 during the construction of a continuous rigid-frame bridge in Guizhou Province and combining this information with measured data, such as crack depth, length, and position, the effects of two extreme remedial measures—complete closure after cracking and nonclosure after cracking—on the structural performance of the entire bridge are analyzed using the finite element software Midas FEA and compared with the originally designed structure without cracking. The analysis results indicate that the structural performance of the completely closed structure after cracking is basically consistent with that of the originally designed undamaged structure. Nonclosure after cracking has a significant impact on the stress distributions of the top and bottom slabs and webs near pier cap block 0, and the stress levels of these components are greater than those of the undamaged model. In this study, the most unfavorable conditions are comprehensively considered, and the influences of bridge cracks during the construction stage on the structural performance of the entire bridge are investigated. This investigation plays an important role in the safety performance evaluation after cracking during the construction of bridges, and it can serve as a practical reference for these tasks.

Citation: Chen, J.; Wang, C.; Shen, Y. Structural Performance Evaluation After Cracking During the Construction of Long-Span Continuous Rigid-Frame Bridges. *Prestress Technology* **2024**, *1*, 41-55. https://doi.org/10.59238/j.pt.2024.01.004

Received: 05/01/2024
Accepted: 26/02/2024
Published: 25/03/2024

Publisher's Note: Prestress technology stays neutral with regard to jurisdictional claims in published maps and institutional affiliations.

Keywords: long-span continuous rigid-frame bridge; construction stage; crack simulation; evaluation of overall bridge structural performance

1 Introduction

With the advancement of the field of infrastructure construction in China, the requirements for the structural performance of bridges are increasing. Cracks may develop in reinforced concrete bridges due to factors such as loading, temperature variation, shrinkage, and steel corrosion, which can compromise the structural safety and durability. According to bridge design specifications, most prestressed concrete bridges are designed as fully or partially prestressed concrete components (Class A components). Prestressed concrete bridges are designed to prevent cracking during the construction and operational stages. However, some prestressed concrete bridges may develop cracks during the construction stage due to factors such as temperature variations or improper construction practices. If these cracks are not addressed, they can reduce structural safety and durability. Therefore, the evaluation technique for cracking during the construction of long-span bridges is crucial for evaluating the safety performance and for decision-making regarding remediation.

Many global scholars have conducted research on the impact of cracks on the bearing capacity of reinforced concrete bridges. Qu et al. [1] established a membership function for crack width related to durability failure, and they proposed a fuzzy probability calculation method for structural durability failure and a predictive assessment method for the future state of concrete bridge durability. Zhang et al. [2] conducted destructive tests on five reinforced concrete rectangular beam models

subjected to graded concentrated loads and determined the relationships among the maximum crack height, average height, crack width, and bearing capacity. The scholars obtained empirical formulas by regression and proposed the use of crack characteristic methods for the rapid detection and evaluation of bridge bearing capacity. Guo et al. [3] verified the feasibility of evaluating the bearing capacity of a reinforced concrete beam by applying the crack width extension evaluation method to a group of simply supported beam models during experiments. Jiao et al. [4] derived a function for the normal serviceability limit state of reinforced concrete bridges based on the maximum crack width and calculated reliable indicators using MATLAB programming. The results showed that the maximum crack width reliable indicator basically met the design requirements. He et al. [5] established a three-dimensional solid damage model to study the damage and bearing capacities of structures under various conditions, such as bending vertical cracking, shear diagonal cracking, crack quantity, concrete reinforcement quantity, steel reinforcement shape, and initial microcracking. Xiang et al. [6] established a multiscale numerical model based on the extended finite element method to reveal the crack propagation mechanism. Zhang et al. [7] used deep learning combined with image classification and semantic segmentation methods to extract information from images to evaluate the state of cracks. Liu et al. [8] conducted an image-based crack assessment of bridge piers using drones and 3D scene reconstruction. Ma et al. [9] combined ABAQUS and FRANC3D to establish a numerical simulation method for corrosion fatigue crack propagation. Kang et al. [10] used an automatic double-sided rebound system for rapid damage assessment of concrete bridge decks.

According to a summary of the existing research on the influence of cracks on bridge performance globally, most of the existing research in China concerned this influence on the structural performance of completed bridges. There is a lack of research on the influence of cracks on the structural performance of bridges during construction. In this paper, the cracking problem of pier cap block 0 (the No. 0 section of the bridge) during the construction of a continuous rigid frame bridge in Guizhou Province is taken as the engineering background. Combined with the measured data of crack depth, length and position, the finite element software Midas FEA is used to analyze the influences of two extreme treatment measures on the structural performance of the whole bridge: complete closure and nonclosure after cracking. A comparison is made with an originally designed structure without cracks to evaluate the structural performance after cracking during the construction phase. Unlike other existing studies, the performance is evaluated once the cracks appear after the bridge is completed. The focus of this study is on the performance evaluation of the whole bridge after cracks appear during the construction stage. An in-depth study of the influence of bridge cracks on the structural performance of the whole bridge during the construction stage can serve as a support case for the performance evaluation of this system. Moreover, this study can provide a practical reference for the evaluation of the performance and the remediation of a whole bridge after cracks appear during the construction stage.

2 Project Overview

The main bridge of a highway bridge in Guizhou Province consists of a 55 m+100 m+55 m three-span prestressed concrete continuous rigid-frame bridge, as shown in the elevation diagram in Figure 1. The width of the single-width bridge is 10.625 m, and the main beam has a single-box single-chamber straight web section made of C50 concrete. The width of the top slab of the box beam is 10.625 m, the width of the bottom slab is 6.0 m, the length of the cantilever is 2.3 m, and the height of the box beam at the root is 6.12 m. The main piers are divided into two parts. The upper part is a separated double-thin-wall pier, and the lower part is an integral box-section pier, both of which are made of C40 concrete. The foundation use drilled grouting piles with C30 underwater concrete. The upper structures of the main bridge are

 https://doi.org/10.59238/j.pt.2024.01.004

constructed by cantilever casting, and the lower piers are constructed by cast-in-place construction.

The division of the left half-span beam section of the right bridge is shown in Figure 2. Cracks appear at the No. 0 blocks (the No. 25 pier and No. 26 pier) of the bridge during the construction stage. The crack depth and width of the No. 0 blocks of the right bridge are detected. The distribution of cracks in the left and right webs of the No. 0 block of the No. 25 pier in the right bridge is shown in Figure 3. The cracks of the pier are mainly concentrated in the web, and they predominantly appear as vertical cracks.

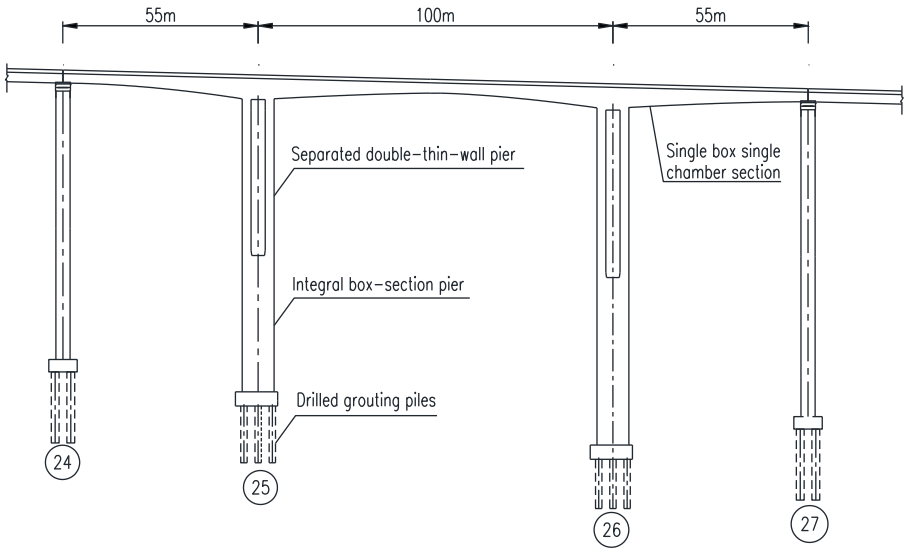

Figure 1 Elevation diagram of the bridge structure

The left half-span of the right single-width section of the bridge is divided as shown in Figure 2. During the construction stage, cracks appear in piers 25 and 26 and block 0. Partial crack depth and width measurements are available for the cracks in block 0 of pier 25 and pier 26 of the right single-width section. The schematic distributions of cracks in the left and right webs of block 0 of pier 25 in the right single-width section are shown in Figure 3, with cracks mainly concentrated in the webs that predominantly appear as vertical cracks.

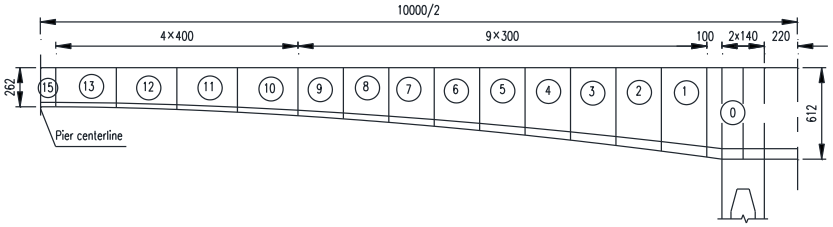

(a) Beam segment division diagram-part 1

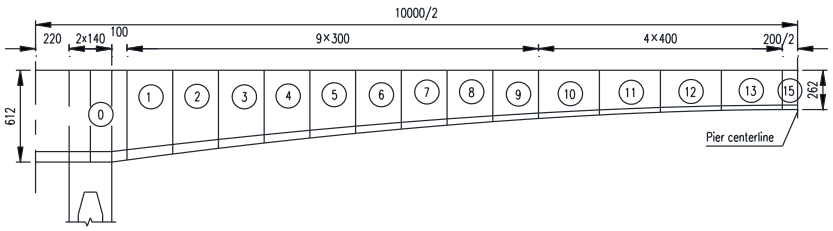

(b) Beam segment division diagram-part 2

Figure 2 Diagram of the division of beam segments (Unit: cm)

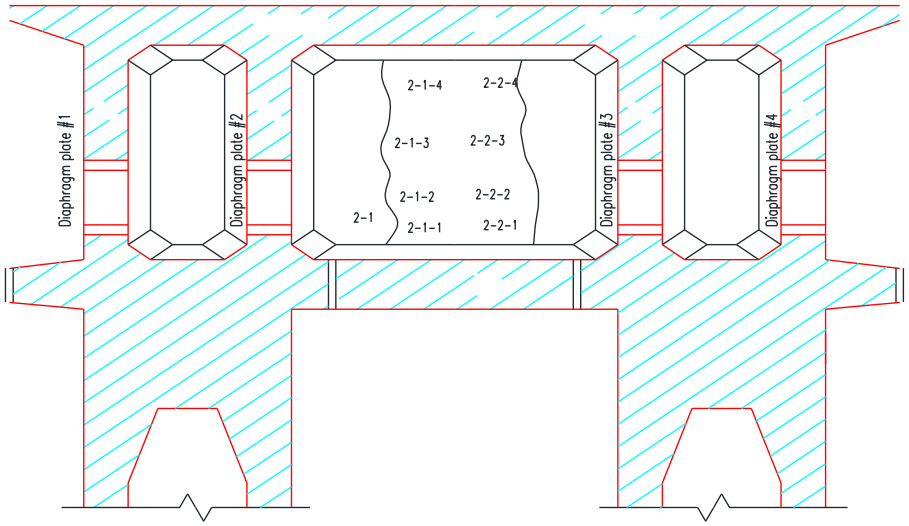

(a) Cracks in the left web of the No. 0 block of the No. 25 pier of the right bridge

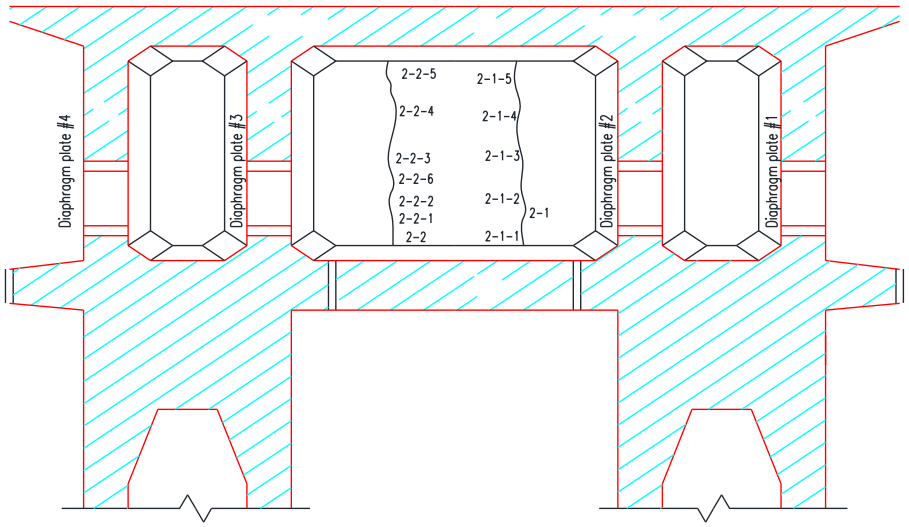

(b) Cracks in the right web of the No. 0 block of the No. 25 pier of the right bridge

Figure 3 Web crack distribution diagrams of the No. 0 block of the No. 25 pier of the right bridge

Due to the cracks in the No. 0 block, the evaluation of the structural performance of the bridge should not be simply conducted as a conventional design review. Additionally, after crack repair, there are three cases: full repair success, partial repair success, and repair failure. The structural and material performance attributes of repaired cracks are challenging to simulate. Therefore, an evaluation method in which finite element models are established is proposed in this paper to analyze the structural performance of bridges under three conditions: undamaged original design, complete closure after cracking, and nonclosure after cracking. The differences among the three cases are compared to effectively evaluate the degree to which the structural performance of the bridge is affected by cracking. This evaluation method considers the most unfavorable conditions, and the analysis cost is low, which can meet the actual needs of engineering construction. The main evaluation process includes the following three aspects:

(1) Analysis of the structural performance during both the construction and operational stages of the originally designed structure without cracks in block 0, i.e., the performance of the undamaged originally designed structure.

 https://doi.org/10.59238/j.pt.2024.01.004

(2) Analysis of the structural performance during both the construction and operational stages of the structure after complete closure following cracking (block 0 cracks occurred during construction, effective repair of block 0 cracks occurred before the construction of bridge section 1), i.e., the performance of the structure after complete closure following cracking.
(3) Analysis of the structural performance during both the construction and operational stages of the structure after nonclosure following cracking (cracks occurred in block 0 during construction and persisted thereafter, i.e., the scenario where crack repair failed), i.e., the performance of the structure after nonclosure following cracking.

3 Bridge Finite Element Model

Considering the fine-scale parameters of cracks in the objects studied, it is necessary to establish a three-dimensional solid finite element model for detailed simulation. Therefore, the three-dimensional solid finite element program Midas FEA was selected for the analysis of the structural performance of the bridge. Based on the evaluation results, finite element models were established for the undamaged state, complete closure after cracking state, and nonclosure after cracking state. Since the main piers and abutments of the bridge were high piers, the shrinkage and creep of the pier body and the settlement of the foundation significantly impacted the overall structural performance. Therefore, the finite element model was used to simulate the pier body, pier cap, and foundation of both the main piers and the abutments and to simulate the construction process. In each finite element model, concrete was represented using solid elements, while three-directional prestressing was represented using prestressed steel tendon elements. The overall bridge solid finite element model is shown in Figure 4.

Figure 4 Bridge finite element model

In this study, the construction process was simulated during finite element modeling analysis, which mainly included five stages: main pier construction, block 0 construction, segment #13 construction (at the maximum cantilever state), side span closure, and middle span closure. The construction process simulation for each stage is shown in Figure 5.

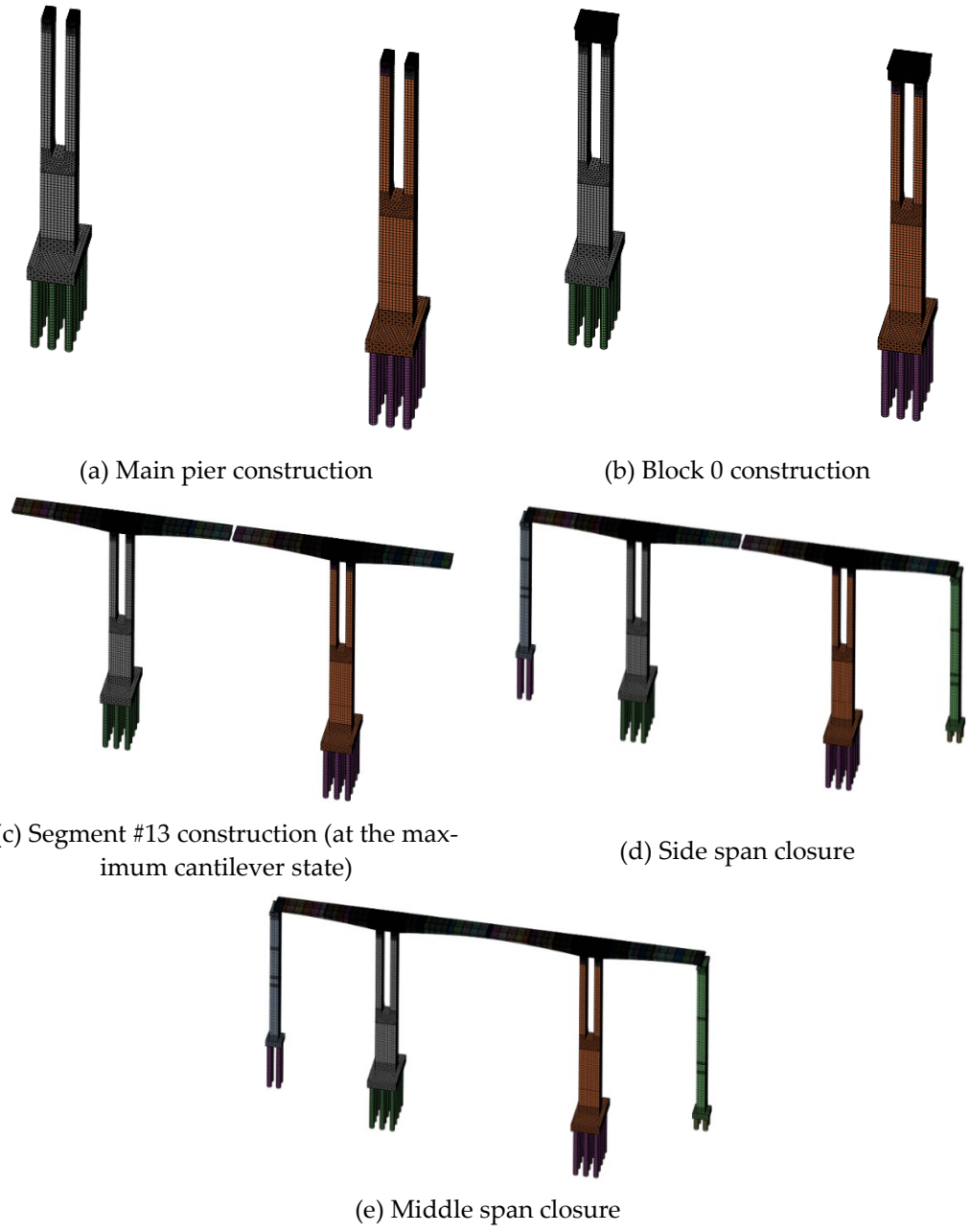

(a) Main pier construction

(b) Block 0 construction

(c) Segment #13 construction (at the maximum cantilever state)

(d) Side span closure

(e) Middle span closure

Figure 5 Construction process of the bridge during analysis

During load simulation, the model primarily considered permanent and variable loads. The permanent loads included self-weight, concrete shrinkage, creep, the second-stage load weight of the bridge deck, and foundation displacement. Conversely, the variable loads included highway class-I vehicle loads, temperature effects, construction loads, and bearing friction. Additionally, the model comprehensively considered the effects of prestressing and concrete shrinkage creep during load simulation.

The finite element crack simulation schematic diagram is shown in Figure 6. The crack simulation in this finite element model adopted the discrete crack model simulation method. Initially, measured data were utilized to determine basic parameters such as the starting point, length, and width of cracks in the model. Then, nodes were created along the crack path, and the crack was treated as a boundary of the elements. New nodes were added, and elements were redefined whenever a new crack appeared. Based on the measured crack data, the main vertical crack positions, lengths,

 https://doi.org/10.59238/j.pt.2024.01.004

depths, and widths inside the middle web of the block 0 crossbeam were simulated. After cracking, a contact element with only compression was used between the crack interfaces to simulate cracking.

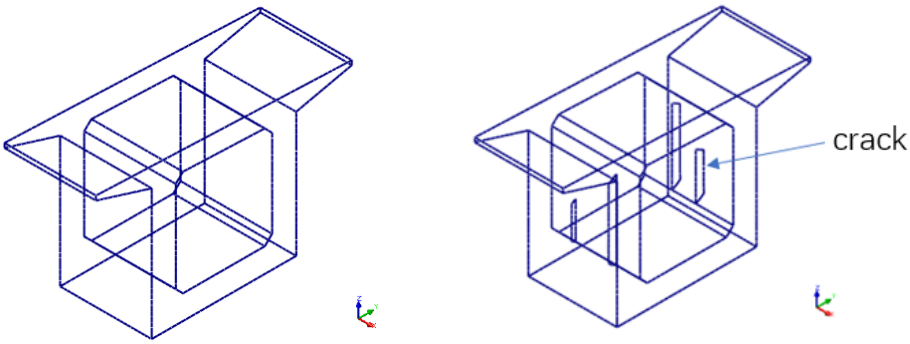

(a) Undamaged model (b) Cracked model

Figure 6 Crack simulation in the finite element model

Among the three models simulated, the models of complete closure after cracking and nonclosure after cracking were both considered cracked models. However, the former finite element model was obtained by modifying the element boundaries to achieve complete closure of the cracks based on the latter model of nonclosure after cracking. The main difference between the model of complete closure after cracking and the undamaged model was that the former model underwent crack simulation before the closure of cracks, whereas the latter model did not undergo discrete crack simulation.

4 Analysis Results

In accordance with the "Specifications for Design of Highway Reinforced Concrete and Prestressed Concrete Bridges and Culverts" (JTG 3362-2018) [11], the stress analysis of the bridge structure under transient conditions, the serviceability limit state analysis under persistent conditions and the stress analysis under persistent conditions are carried out. Due to space limitations, only the influence of No. 0 block cracking of the No. 25 pier on the structural performance of the whole bridge is analyzed in this paper. The specific analysis results are as follows:

4.1 Stress Analysis of the Transient Conditions

The stress analysis of transient conditions mainly considers two working conditions: after the completion of block 0 construction and during the maximum double cantilever stage of the construction phase.

The distribution of the normal stress in the concrete of block 0 on pier 25 after the completion of block 0 construction is shown in Figure 7. Under self-weight and prestressing loads, the prestress transfer path of the undamaged model is good, with the maximum tensile stress being less than 0.35 MPa. The stress distribution of the model after complete closure following cracking is essentially consistent with that of the undamaged model. However, in the nonclosure after cracking model, due to the influence of cracks in the web, compressive stress cannot be effectively transferred through the web, resulting in higher compressive stress levels in the top slab than those in the undamaged model; furthermore, the stress becomes increasingly concentrated.

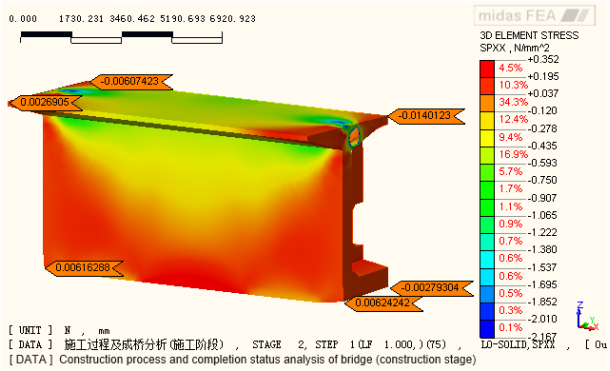

(a) Undamaged model

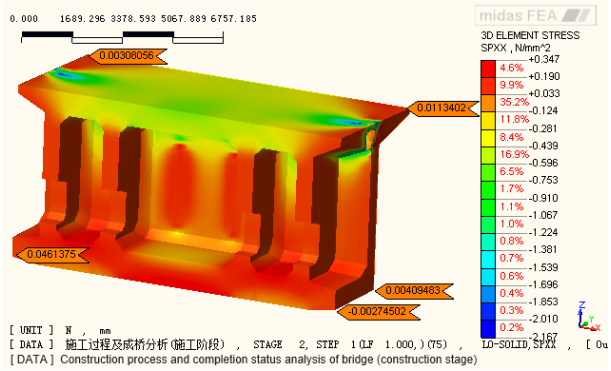

(b) Complete closure after cracking model

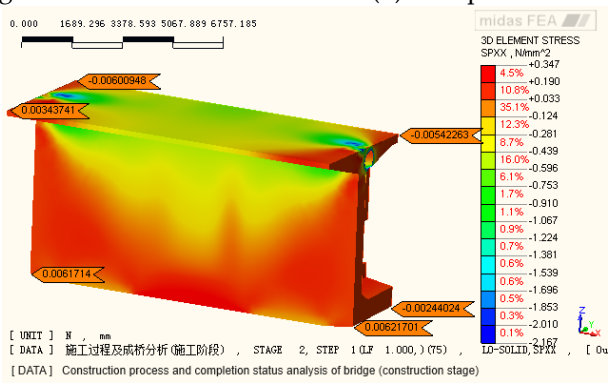

(c) Nonclosure after cracking model

Figure 7 Normal stress distribution in the No. 0 block concrete of the No. 25 pier (Unit: MPa)

During the maximum double cantilever stage of the construction phase, the distributions of the normal stresses in the concrete of the bridge top and bottom slabs along the span are shown in Figure 8. The distributions of normal stresses in the concrete of the top and bottom slabs of the model after complete closure following cracking are almost identical to those of the undamaged model. However, in the nonclosure after cracking model, the stresses of the top and bottom slabs of the structure receive a certain impact during this construction phase. In the nonclosure after cracking model, there is a maximum increase of 1.66% in the normal stress near the top slab and a maximum increase of 7.68% in that near the bottom slab of pier block 0. The stress distributions of the top and bottom slabs at other positions are basically consistent with those of the undamaged model.

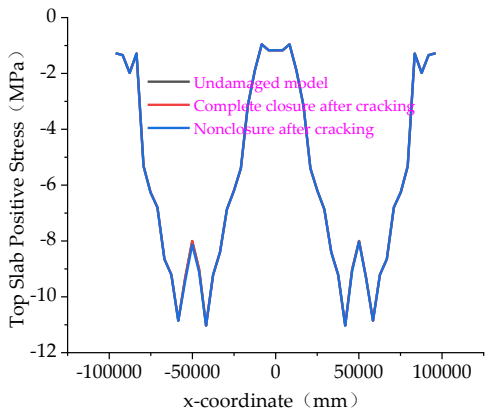

(a) Normal stress distribution of the top slab

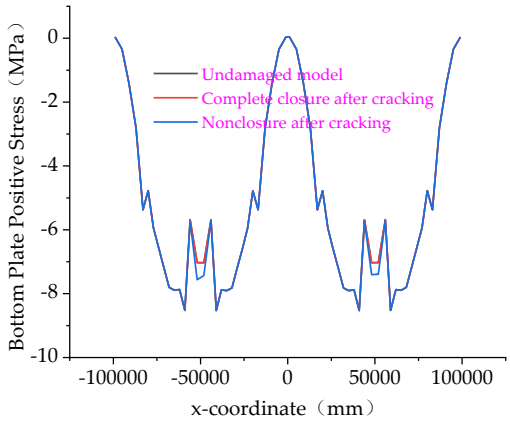

(b) Normal stress distribution of the bottom slab

Figure 8 Normal stress distributions of the top and bottom slabs along the longitudinal direction of the bridge during the maximum double cantilever stage

https://doi.org/10.59238/j.pt.2024.01.004

Table 1 Normal stresses of the top and bottom slabs during the maximum double cantilever stage (Unit: MPa)

Stress category	Model coordinate (m)	Undamaged model	After complete closure following cracking	After nonclosure following cracking	Ratio (complete closure/undamaged)	Ratio (nonclosure/undamaged)
Top slab stress	-50.13	-8.00	-8.00	-8.13	100.05%	101.66%
Bottom slab stress	-51.90	-7.02	-7.03	-7.56	100.14%	107.68%

4.2 Normal Serviceability Limit State Analysis

4.2.1 Initial and Later Permanent Loads in the Completed Bridge

Under the initial permanent loads of the completed bridge, the stress distributions of the top and bottom slabs along the longitudinal direction of the bridge for the three models are shown in Figure 9. The stress distributions of the top and bottom slabs in the model after complete closure following cracking are almost consistent with those of the undamaged model. However, in the nonclosure after cracking model, compared to the undamaged model, only a 1.67% increase in the normal stress near the top slab and an 8.94% maximum increase in that near the bottom slab of block 0 are observed. The stress states at other positions outside the area affected by pier cracking are consistent with those of the undamaged model.

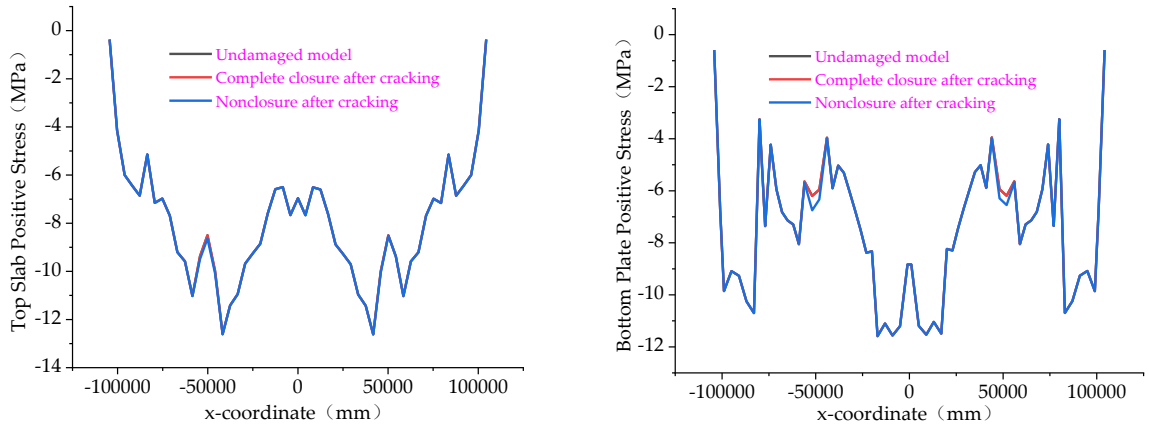

(a) Stress distributions of the top slabs (b) Stress distributions of the bottom slabs

Figure 9 Diagram of the stress distributions of the top and bottom slabs along the longitudinal direction under permanent loads in the initial stage of bridge completion

Table 2 Normal stresses in the top and bottom slabs during the initial stage after bridge completion under permanent loading (Unit: MPa)

Stress category	Model coordinate (m)	Undamaged model	After complete closure following cracking	After nonclosure following cracking	Ratio (complete closure/undamaged)	Ratio (nonclosure/undamaged)
Top slab stress	-50.13	-8.50	-8.50	-8.64	100.04%	101.67%
Bottom slab stress	-51.90	-6.20	-6.20	-6.75	100.15%	108.94%

Under the later permanent load of the completed bridge, the stress distributions of the top and bottom slabs along the longitudinal direction for the three models are shown in Figure 10. The stress distributions of the top and bottom slabs in the model after complete closure following cracking are essentially consistent with those of the undamaged model. However, in the nonclosure after cracking model, compared to the undamaged model, only a 1.58% increase in the normal stress near the top slab and an 8.77% maximum increase in that near the bottom slab of block 0 are observed.

The stress states at other positions outside the area affected by pier cracking remain consistent with those of the undamaged model.

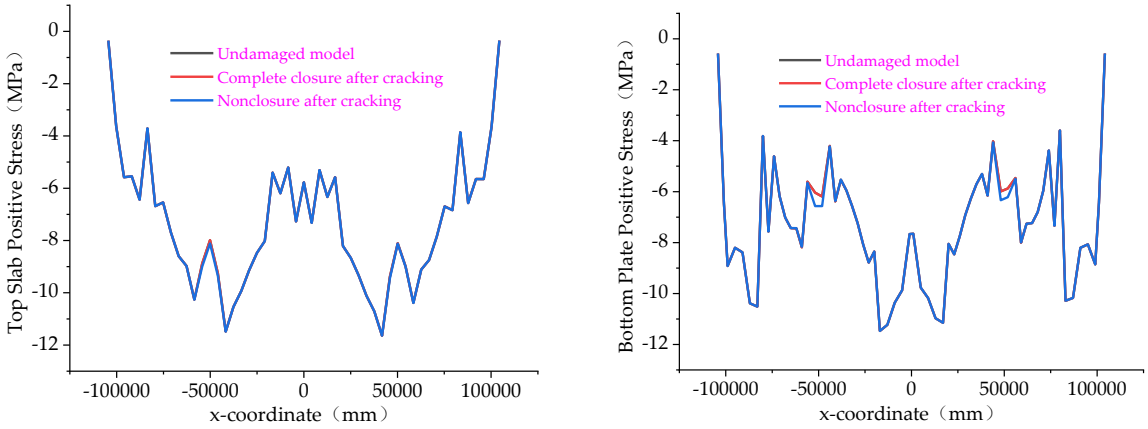

(a) Stress distributions of the top slabs (b) Stress distributions of the bottom slabs

Figure 10 Diagrams of the stress distributions of the top and bottom slabs along the longitudinal direction under permanent loads in the later stage of bridge completion

Table 3 Normal stresses in the top and bottom slabs during the later stage after bridge completion under permanent loading (Unit: MPa)

Stress category	Model coordinate (m)	Undamaged model	After complete closure following cracking	After nonclosure following cracking	Ratio (complete closure/undamaged)	Ratio (nonclosure/undamaged)
Top slab stress	-50.13	-7.99	-7.99	-8.12	100.00%	101.58%
Bottom slab stress	-51.90	-6.04	-6.04	-6.57	100.01%	108.77%

4.2.2 Positive Cross-Section Cracking of the Main Girder Block 0 Under Persistent Situation

The distribution of compressive stresses on the inner side of the web plate of Pier 25 Block 0 under frequent combination of actions are shown in Figure 11. The distributions of compressive stresses on the inner side of the web plate for both the uncracked model and the complete closure after cracking model are essentially consistent. However, the model with nonclosure cracking exhibits significant differences from the uncracked model due to the presence of permanent cracks on the web plate of Block 0. These differences are mainly manifested in three aspects. First, the compressive stress cannot be effectively transmitted at the crack, resulting in a nonlinear distribution of compressive stress at the crack position, with significant discontinuities in the compressive stress at the upper and lower edges of the crack. Second, there is a concentration of compressive stress at the upper edge of the crack in the web plate with a maximum value of -14.04 MPa. Third, the transmission performance of the web plate in the crack area is somewhat affected, with the influence of the crack on the transmission of force in the longitudinal direction being approximately half the height of the crack.

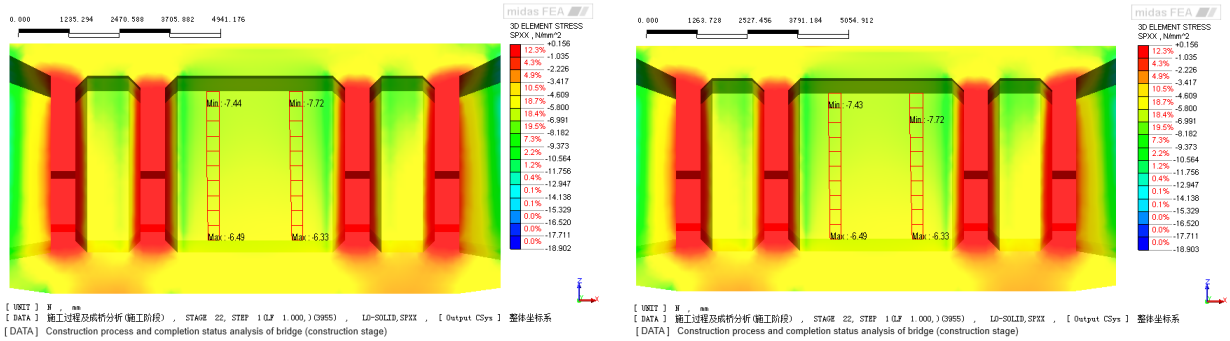

(a) Undamaged model (b) Complete closure after cracking model

https://doi.org/10.59238/j.pt.2024.01.004

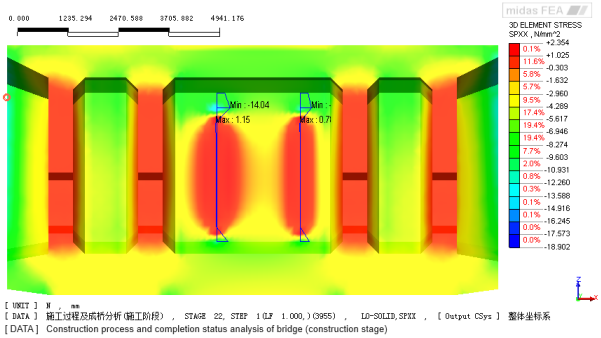

(c) Nonclosure after cracking model

Figure 11 Distribution of the compressive stress on the inner side of the web plate of Pier 25 Block 0 (Unit: MPa)

The distributions of the principal tensile stresses in the web concrete plates of the three models along the longitudinal direction of the bridge under frequent combination of actions are shown in Figure 12. The principal tensile stresses in the slabs of the complete closure after cracking model are essentially consistent with those of the uncracked model. However, in the nonclosure after cracking model, there is only a slight increase in the maximum principal tensile stress (0.061 MPa) in block 0, while the stress distributions at other positions are largely consistent with those in the uncracked model.

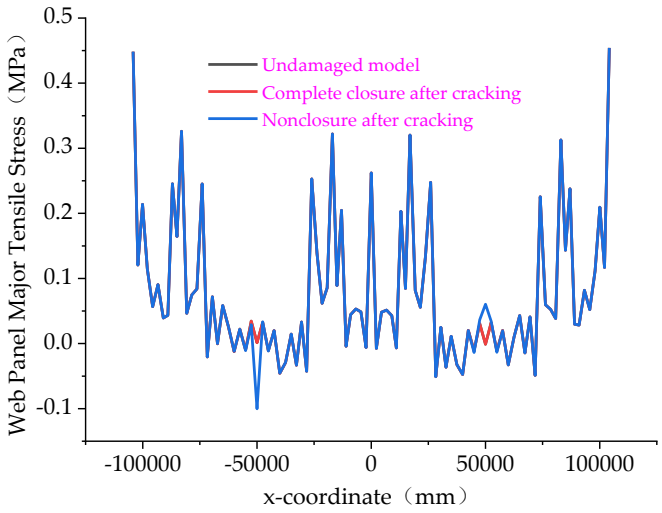

Figure 12 Principal tensile stress distributions in the web plate along the longitudinal direction

4.3 Permanent Situation Stress Analysis

Under the fundamental combination of actions, the distributions of normal stresses in the top and bottom concrete slabs along the longitudinal direction of the bridge and in the concrete of block 0 for the three models are shown in Figure 13 and Figure 14, respectively. The distribution of stresses in the complete closure after cracking model is generally consistent with that of the uncracked model. The presence of cracks has a certain influence on the distribution of normal stress at the concrete of block 0 near the pier top; this influence is specifically manifested in the form of localized stress concentrations at the upper and lower edges of the cracks. Relative to the uncracked model, the nonclosure after cracking model has a 1.81% increase in normal stress at the top slab and a 7.53% increase at the bottom slab of block 0.

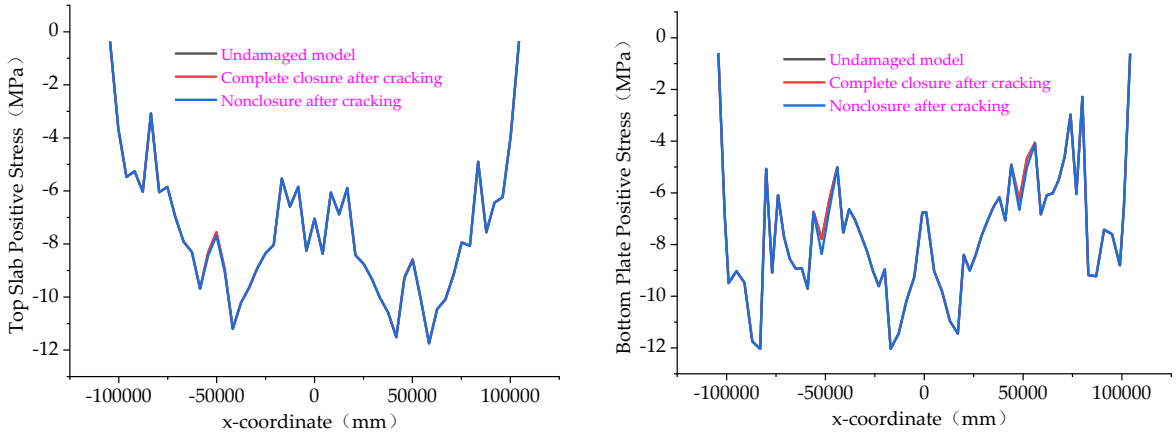

(a) Normal stress of the top slab (b) Normal stress of the bottom slab

Figure 13 Normal stress distributions of the top and bottom concrete slabs along the longitudinal direction

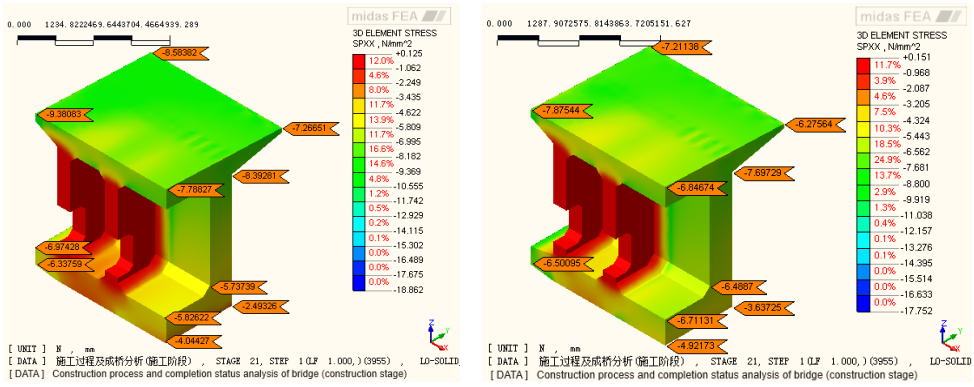

(a) Undamaged model (b) Complete closure after cracking model

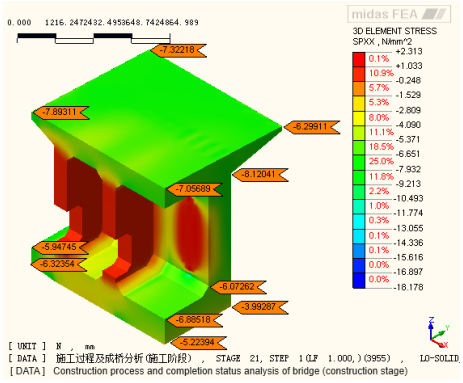

(c) Nonclosure after cracking model

Figure 14 Distributions of the normal stress in the concrete of block 0 (Unit: MPa)

Under the fundamental combination of actions, the distributions of the principal compressive stresses in the concrete slab along the longitudinal direction of the bridge and in the concrete of block 0 are shown in Figures 15 and 16, respectively. The distributions of the principal compressive stresses in the slab and block 0 in the complete closure after cracking model are generally consistent with those in the uncracked model. However, relative to the uncracked model, the nonclosure after cracking model exhibits an increase in the principal compressive stress in the web plate near the bridge piers, which is particularly evident in the principal compressive stress at the bottom slab of block 0 near the pier top. There is a 6.31% increase in the principal compressive stress, and localized stress concentrations can be observed at

 https://doi.org/10.59238/j.pt.2024.01.004

the upper and lower edges of the cracks. The distribution of the principal compressive stress in other locations of the nonclosure after cracking model remains largely consistent with that of the uncracked model.

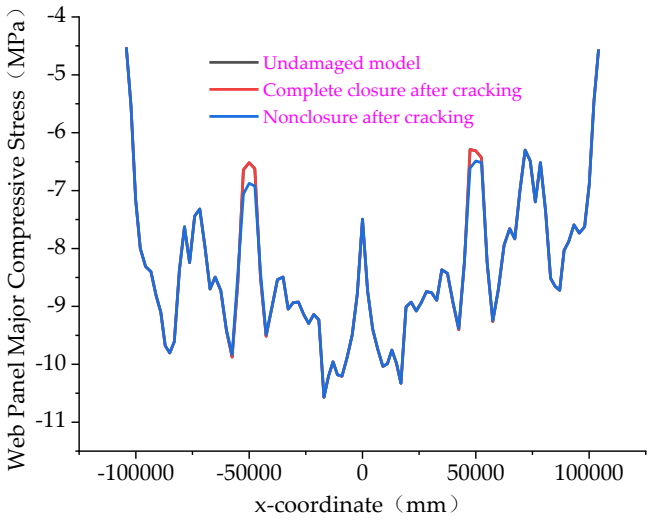

Figure 15 Principal compressive stress distribution of the concrete web plate

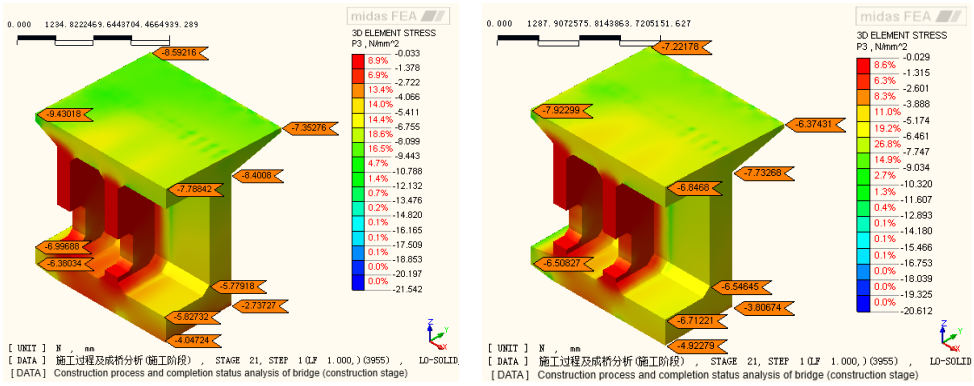

(a) Undamaged model (b) Complete closure after cracking model

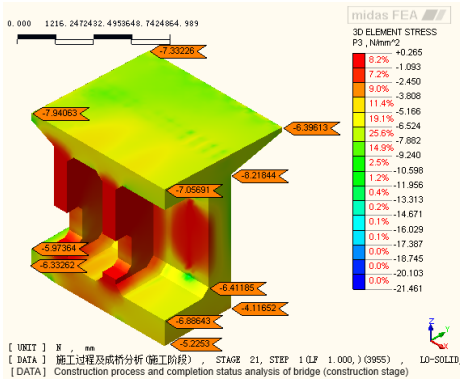

(c) Nonclosure after cracking model

Figure 16 Distribution of the principal compressive stress in the concrete of block 0 (Unit: MPa)

5 Conclusions

In this study, which was based on a real engineering case of cracking in bridge piers during construction, Midas FEA software was utilized to establish three scenarios for modeling an entire bridge: uncracked, complete closure after cracking, and nonclosure after cracking. The objective was to evaluate the impact of cracks during

the construction phase on the overall structural performance of the bridge. The following conclusions were drawn:

(1) The complete closure after cracking model exhibited concrete stress distributions under both temporary and permanent conditions that were almost identical to those of the uncracked model. This similarity suggested that the overall structural performance of the bridge could be restored to that of the original design after effectively repairing the pier cracks.
(2) The cracks mainly have a certain influence on the stress distributions of the top and bottom slabs and webs near the No. 0 block of the pier top. Compared with those in the uncracked model, significant increases in stress levels were observed in the top and bottom slabs and webs near block 0 in the nonclosure after cracking model.
(3) This evaluation method, which considered the worst-case scenario and had low analysis costs, could meet the practical requirements of engineering construction. Thus, this study could serve as a reference for subsequent engineering practices.

In summary, the results of this study are important for evaluating the impact of bridge structure cracks on the overall structural performance during the construction phase. This study provides valuable case support and practical guidance for evaluating overall bridge performance after cracking during construction.

Conflict of Interest: All authors disclosed no relevant relationships.

Data Availability Statement: The data that support the findings of this study are available from the corresponding author, Chen, upon reasonable request.

References

1. Qu, W.; Che, H. Evaluation of Concrete Bridge Durability on Concrete Crack. *Journal of the China Railway Society* **1997**, *19*, 91-99.
2. Zhang, W.; Liu, X.; Luo, B.; Li, M. Quick Assessment of Loading Capacity of Bridge by Cracking Characteristics. *Journal of Northeastern University(Natural Science)* **2008**, 1346-1349, doi:10.3321/j.issn:1005-3026.2008.09.032.
3. Guo, H. Research on Evaluation for Bearing Capacity of Reinforced Concrete Bridges Based on Extension of Crack Width. *Technology of Highway and Transport* **2010**, 58-62, doi:10.3969/j.issn.1009-6477.2010.01.016.
4. Jiao, M.; Sun, L. Reliability of Reinforced Concrete Bridge Girder Based on Maximum Crack Width. *Engineering Mechanics* **2010**, *27*, 245-249.
5. He, Y. The Research on Calculation Method and Damage Evalution of Bridges based on the Charateristic of Cracks Distribution. Hebei University of Technology, 2015.
6. Xiang, Z.; Zhu, Z.W.; Lei, X.N. Fatigue Assessment and Crack Propagation of Floorbeam Cutout in Orthotropic Bridge Decks. *Mater Design* **2023**, *226*, doi:10.1016/j.matdes.2023.111676.
7. Zhang, X.; Wogen, B.E.; Liu, X.Y.; Iturburu, L.; Salmeron, M.; Dyke, S.J.; Poston, R.; Ramirez, J.A. Machine-Aided Bridge Deck Crack Condition State Assessment Using Artificial Intelligence. *Sensors-Basel* **2023**, *23*, doi:10.3390/s23094192.
8. Liu, Y.F.; Nie, X.; Fan, J.S.; Liu, X.G. Image-Based Crack Assessment of Bridge Piers Using Unmanned Aerial Vehicles and Three-Dimensional Scene Reconstruction. *Comput-Aided Civ Inf* **2020**, *35*, 511-529, doi:10.1111/mice.12501.
9. Ma, Y.F.; He, Y.; Wang, G.D.; Wang, L.; Zhang, J.R.; Lee, D. Corrosion Fatigue Crack Growth Prediction of Bridge Suspender Wires Using Bayesian Gaussian Process. *Int J Fatigue* **2023**, *168*, doi:10.1016/j.ijfatigue.2022.107377.

 https://doi.org/10.59238/j.pt.2024.01.004

10. Kang, S.G.; Wu, Y.C.; David, D.S.; Ham, S. Rapid Damage Assessment of Concrete Bridge Deck Leveraging an Automated Double-Sided Bounce System. *Automation in Construction* **2022**, *138*, doi:10.1016/j.autcon.2022.104244.
11. Ministry of Transport of the People's Republic of China JTG 3362—2018 Specifications for Design of Highway Reinforced Concrete and Prestressed Concrete Bridges and Culverts. China Communications Press: Beijing, 2018.

AUTHOR BIOGRAPHIES

Jiasi Chen

M.E. Department of Bridge Engineering, Tongji University.

Research Direction: Prestressed Concrete Bridge.

Email: 2132483@tongji.edu.cn

Chengyue Wang

M.E. Department of Bridge Engineering, Tongji University.

Research Direction: Prestressed Concrete Bridge.

Email: 846898486@qq.com

Yin Shen

D.Eng, Associate Professor. Department of Bridge Engineering, Tongji University.

Research Direction: Prestressed Concrete Bridges, Prefabricated and Assembled Bridges and Long-span Bridges.

Email: shenyin@tongji.edu.cn